Hindawi Publishing Corporation
Journal of Chemistry
Volume 2014, Article ID 150256, 9 pages
http://dx.doi.org/10.1155/2014/150256

Research Article

A Study on the Morphology of a Dispersed Particle Gel Used as a Profile Control Agent for Improved Oil Recovery

Qing You,[1,2,3] Yongchun Tang,[4] Caili Dai,[5] Mingwei Zhao,[5] and Fulin Zhao[5]

[1] *School of Energy Resources, China University of Geosciences, Beijing 100083, China*
[2] *Key Laboratory of Marine Reservoir Evolution and Hydrocarbon Accumulation Mechanism, Ministry of Education, China University of Geosciences, Beijing 100083, China*
[3] *Key Laboratory of Shale Gas Exploration and Evaluation, Ministry of Land and Resources, China University of Geosciences, Beijing 100083, China*
[4] *Power, Environmental and Energy Research Institute, Los Angeles, CA 91722, USA*
[5] *School of Petroleum Engineering, China University of Petroleum, Qingdao, Shandong 266580, China*

Correspondence should be addressed to Qing You; youqing@cugb.edu.cn

Received 15 April 2014; Accepted 27 June 2014; Published 20 July 2014

Academic Editor: Yu Xin Zhang

To achieve in-depth profile control of injection water and improve oil recovery, a new profile control agent, termed as dispersed particle gel (DPG), has been developed and reported. In this paper, the morphology of DPG and the factors that influence its morphology are systematically investigated using atomic force microscopy (AFM). The AFM studies show that DPG is composed of small pseudospherical particles and that their sizes can be controlled by adjusting the shearing rate, the initial polymer mass concentration, and the salinity. Dynamic light scattering (DLS) is used to study the effects of the initial polymer mass concentration, the shearing rate, the salinity, and the high-temperature aging on the particle size of DPG. The aggregation ability of DPG is explained using the DLVO theory and space stability theory. This work provides a scientific basis and technical support for the formula design of DPG and its application in the oil and gas field.

1. Introduction

Oil and gas, as efficient sources of energy, play an important role in the world's economy. With the rapid growth of the world economy, the demand for oil and gas is on the rise. Exploration has become more difficult in recent years, which makes it necessary to improve oil and gas recovery. Moreover, the long-term flooding of oilfields has resulted in the fast injection of water into the oil wells along the high-permeability zones and a dramatic reduction in oil production. Reducing the water production rate is a key to stabilizing and increasing oil production.

Until now, the most effective method of reducing the water production rate is to use profile control agents to block high-permeability zones. The widely adopted profile control agents include bulk gels, colloidal dispersion gels, and polymer gel microspheres, such as bright water, microgels, preformed particle gels, and soft gels. However, these different gels all have limited application in practice. The bulk gel is easily affected by shearing from ground equipment and porous media, by chromatographic separation effect, by dilution from the formation water, and by touch physical and chemical conditions (temperature, pressure, and salinity) in formation; thus, it is hard to control the gelation time, gel strength, and the entering-formation depth of the gel when using bulk gel in a field test [1]. The colloidal dispersion gel [2], polymer gel microsphere [3, 4], microgel [5–7], preformed particle gel, and soft gel [8–10] are all expensive, which inhibits the large-scale application. Therefore, a new in-depth profile control agent that can achieve deep plugging with good stability, control the injection of water, and improve oil recovery needs to be developed.

Because of the problems with the existing profile control agents, it is necessary to develop a new profile control agent. A dispersed particle gel (DPG) that was prepared using the shearing cross-linking method in pipe flow with a polymer

and a cross-linker was designed as a new in-depth profile control agent and has been previously reported [11]. The strength and particle size of DPG are controllable with a particle size distribution from nanometers to millimeters. DPG is not sensitive to reservoir conditions, is environmentally friendly, and is low cost. According to the lab core test results, DPG can block large formation channels and modify the flow profile to achieve a deep profile control effect that diverts water to middle-to-low permeability zones, thus improving the sweep efficiency as well as the oil recovery ratio [12].

DPG is an excellent profile control agent with much potential to solve the problem of a high water cut; therefore, the systematic study of its characteristics has significant practical value. The morphology of DPG, including the shape and particle size, should be studied first because it is the fundamental property of the material. The morphology of DPG and the factors that influence the morphology are studied in this paper to provide a scientific basis and technical support for its IOR mechanism and its application in the field.

2. Materials and Methods

2.1. Materials

Polymer. The hydrophobically associating polymer is from ChemEOR Inc. Its relative molecular weight is 8.0×10^6, its degree of hydrolysis is 26.65%, its solid content is 94%, and its water-insoluble material is 0.24%.

Cross-Linker. Chromium acetate is also from ChemEOR Inc.

DPG Samples. The DPG samples are prepared as previously described [11]. Briefly, first prepare the gelants that are composed of polymer and cross-linker. Then, use a peristaltic pump as the shearing cross-linking equipment to prepare DPG using a certain shearing rate for 2 to 3 hours at room temperature. Adjust the shearing parameters (shearing rate and tube diameter size) and the polymer concentration to obtain a series of DPG products of various sizes. The formation process and formation mechanism in peristaltic pump are shown in Figures 1 and 2.

2.2. Methods

2.2.1. Morphology of DPG. First, dilute the DPG sample to 1000 mg·L^{-1} and pipette 2.0 mL of the DPG sample onto a freshly stripped mica chip (2 cm × 2 cm). Wait for 2 minutes to allow DPG to adhere to the mica chip; then flush the DPG sample one or two times with ultrapure water and dry it immediately with nitrogen. Observe the morphology of the DPG sample at room temperature (25.0 ± 0.1°C) using a Veeco Nanoscope IIIa multifunctional atomic force microscopy (AFM) instrument in tapping mode.

2.2.2. Particle Size of DPG. First, place the sample needle at the bottom of the sample pool. Then, place 1.0 mL of the DPG sample into the sample pool while slowly lifting the sample needle to avoid the formation of bubbles. Next, use a dynamic light scattering (DLS) device (Malvern Zetasizer Nano S) to determine the particle size of DPG. Test temperature is 25°C, scattering angle is 173°, and incident light wave length is 633 nm.

3. Experimental Results

3.1. Morphology of DPG and the Influencing Factors

3.1.1. The Effect of the Polymer Mass Concentration on the Morphology of DPG. Because the DPG solution is a homogeneous phase and is transparent, it is difficult to observe its morphology using an optical microscope. In this work, AFM is used to observe the morphology of DPG.

Figure 4 shows the morphologies of the DPG samples that were formed using polymer and cross-linking agent. As observed in Figure 3, the shape of DPG in aqueous solution is spherical, and the particles are small; the average particle size of DPG increases slightly with the initial polymer mass concentration [13].

Figure 3(a) shows that the long axis of the DPG sample is approximately 0.5 μm and the short axis of the DPG sample is approximately 0.4 μm, with the axial ratio close to 1. During the process of shearing and cross-linking in pipe flow, the gelation system flows in a certain direction, and there is shear action perpendicular to the direction of flow. If the gel deformation cannot withstand the shearing action during the process, the gel will be broken into small pieces. The cross-linking ability in the direction of flow is greater than that in the vertical direction. As the shearing rate increases, the cross-linking ability in the direction of flow becomes weak, which makes the cross-linking abilities in the two directions (parallel to the flow and vertical to the flow) becoming more balanced; thus, the DPG particles obtain a globular shape. Figure 3(b) shows that the long axis of the DPG sample is approximately 0.9 μm and the short axis is approximately 0.7 μm, with the axial ratio close to 1. The particle size has increased compared to Figure 3(a). The size of the polymer molecules and their cross-linking ability increase with the polymer concentration. Therefore, given the same shear force conditions, the particle size of DPG is larger at higher polymer concentration.

To verify the AFM results, the particle size of DPG is also measured. The sedimentation method, static light scattering method, screening method, image method, resistance method, scraper method, settlement bottles method, ventilation method, ultrasonic method, and DLS method are all widely used to determine particle size. Because the DPG solution is an isotropic aqueous solution, its scattered light signal, when determined using a laser particle size analyzer, is too weak to generate an accurate measurement of the particle size. The DLS method has the advantages of rapid measurement process, high detection sensitivity, real-time monitoring of samples, easy sample preparation with no special treatment, and the absence of interference with the nature of the sample during the measurement process. Therefore, the DLS method is preferred in determining the hydrodynamic diameter of DPG and its distribution.

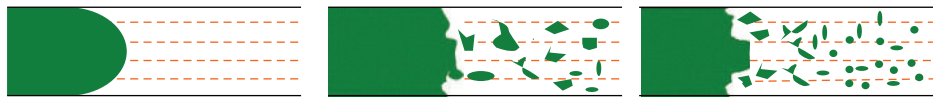

Figure 1: The formation process of DPG in peristaltic pump.

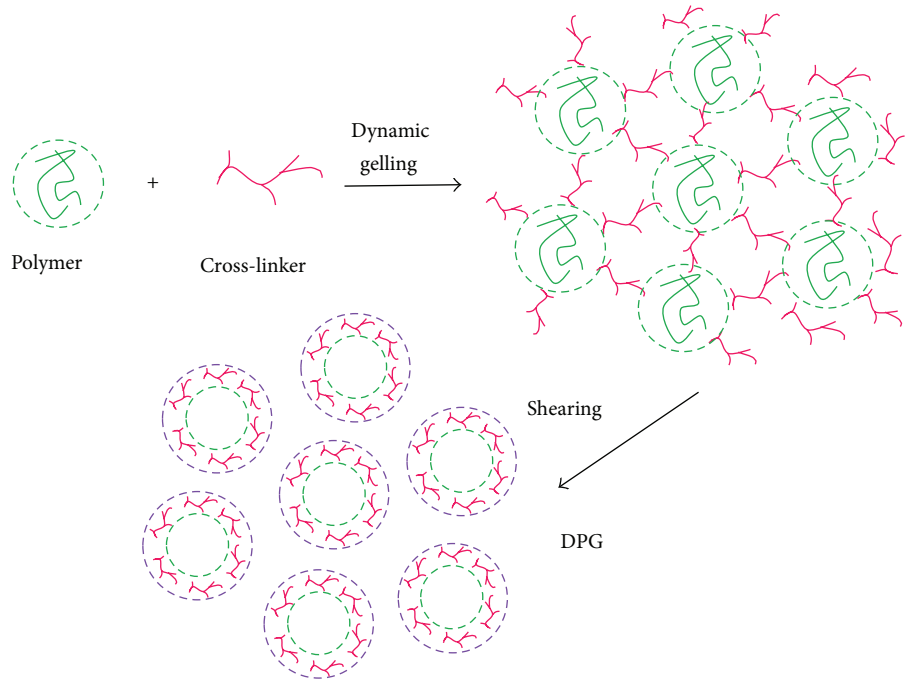

Figure 2: The proposed formation mechanism of DPG.

The particle size distribution curves of the two DPG samples with different initial polymer mass concentrations (shown in Figure 3) are determined using DLS and shown in Figure 4.

There are still two peaks in the particle size distribution curves. Weighted average particle sizes of over 200 nm are obtained using the volume percentages and formula (1), which describes the relationship between the hydrodynamic diameter of a DPG sample and the initial polymer mass concentration, the values of which are given in Table 1. Consider

$$d = \frac{\sum (d_i \cdot i)}{\sum i}, \tag{1}$$

where d is the weighted average particle size in nm, i is the distribution intensity with the d_i particle size as the upper limit, and d_i is the particle size in nm.

As observed in Table 1, the average particle size of DPG increases with the initial polymer mass concentration. A high polymer mass concentration results in a faster rate of cross-linking during the shearing and cross-linking reactions. The amount of cross-linking increases and makes the particle more difficult to cut into pieces and therefore larger.

According to the rupture criteria of DPG [14], under the same shearing rate conditions, the torque generated by the gyration radius R_a of DPG in a polymer solution with a viscosity of η_p is equal to the torque generated by the gyration radius R_p of DPG in a polymer solution with a viscosity of η_a, as described in (2) and (3). Consider

$$\eta_p \gamma R_a^3 = \eta_a \gamma R_p^3, \tag{2}$$

$$\frac{\eta_a}{\eta_p} = \left(\frac{R_a}{R_p}\right)^3. \tag{3}$$

According to (2) and (3), a higher initial viscosity results in a larger particle size of DPG. There is a certain ratio between the initial viscosity and the initial polymer mass concentration, and the experimental results are consistent with the theoretical analysis.

Table 1: Relationship between the particle size of DPG and the initial polymer mass concentration.

Items	Sample	
	1	2
Initial polymer mass concentration/(mg·L^{-1})	3000	4000
Particle size of DPG/nm	1100	1850

3.1.2. Effect of Shearing Rate on the Morphology of DPG. The morphology of DPG formed from 3000 mg·L^{-1} polymer and

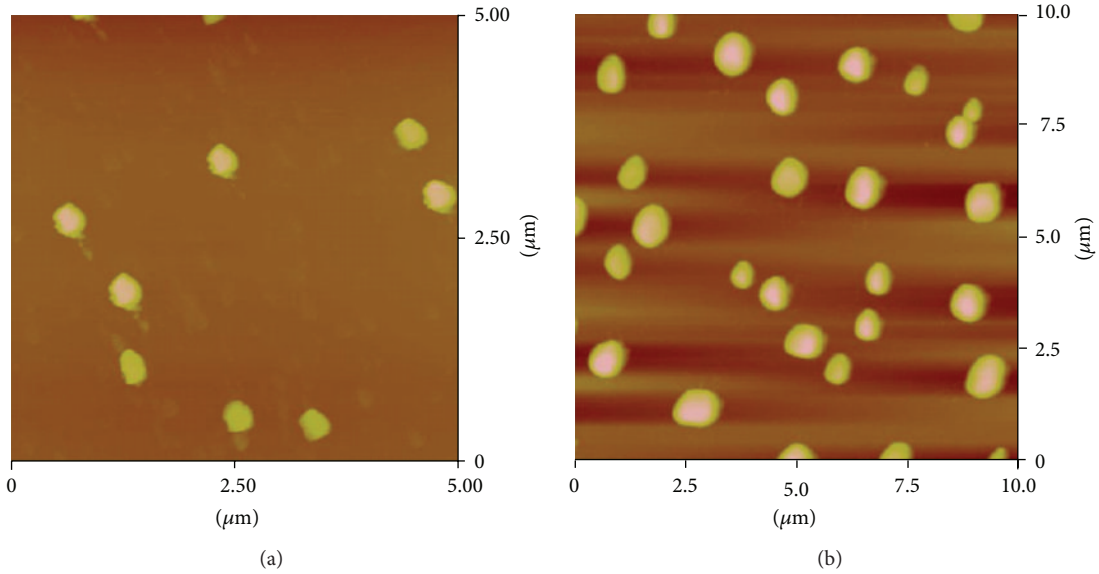

FIGURE 3: AFM image of DPG prepared using different initial polymer mass concentrations. (The scanned area in Figures 3(a) or 3(b) is 5 × 5 μm.) (a) 3000 mg·L^{-1} polymer + 500 mg·L^{-1} $Cr(Ac)_3$; (b) 4000 mg·L^{-1} polymer + 500 mg·L^{-1} $Cr(Ac)_3$.

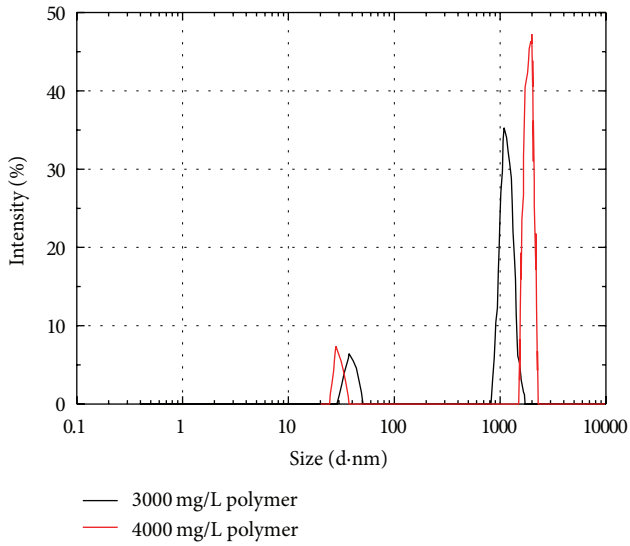

FIGURE 4: Particle size distribution curves of DPG with two different initial polymer mass concentrations.

500 mg·L^{-1} $Cr(Ac)_3$ was studied at average shearing rates of 194 s^{-1} and 168 s^{-1} at 30°C. The results are shown in Figure 5.

As observed in Figure 5, the size of DPG increases when the shearing rate decreases from 194 s^{-1} to 168 s^{-1}, and the morphology becomes less spherical. As the shearing rate increases, the cross-linking ability in the flow direction decreases, which results in a reduction difference of cross-linking ability between the direction of flow and the vertical direction. The cross-linking abilities tend toward balance, which makes the shape of the DPG particles closer to spherical.

Figure 5(b) shows that the distribution of the particle sizes is heterogeneous. Compared with Figure 5(a), the shearing rate in Figure 5(b) is smaller, and the cross-linking ability in the direction of flow is greater than that in the vertical direction. Thus, the particle size of the prepared DPG particles is heterogeneous. A trend towards aggregation in the DPG system also emerges, which is mainly caused by a mutual effect among the DPG particles.

The aggregation phenomenon indicates that the stability of DPG is poor and that DPG is generally characterized by its aggregation stability. According to the DLVO theory, the aggregation stability of DPG in certain conditions is determined by its gravitation and repulsion. When the repulsion surpasses the gravitation, the system is stable and vice versa. The gravitation between particles is essentially the van der Waals force. With two spherical particles of the same size, the gravitational potential energy is given by

$$E_A = -\frac{Aa}{12H}, \tag{4}$$

where E_A is the gravitational potential energy, A is the Hamaker constant, a is the radius of each particle, and H is the shortest distance between the two particles.

In (4), the minus sign means that gravitational potential energy has a positive correlation with the particle size.

The repulsion between the colloidal particles is an electrostatic repulsion generated by the diffuse electric double layers around the particles. With two spherical particles of the same size, the repulsive potential energy ER is generally given by

$$E_R = \frac{64\pi a n_0 kT\gamma_0^2}{K^2} \exp(-KH), \tag{5}$$

where E_R is the repulsive potential energy, a is the radius of each particle, H is the shortest distance between the two particles, K is the reciprocal of the thickness of the diffuse electric double layers, n_0 is the total ion concentration of the system, k is the Boltzmann constant, T is the absolute

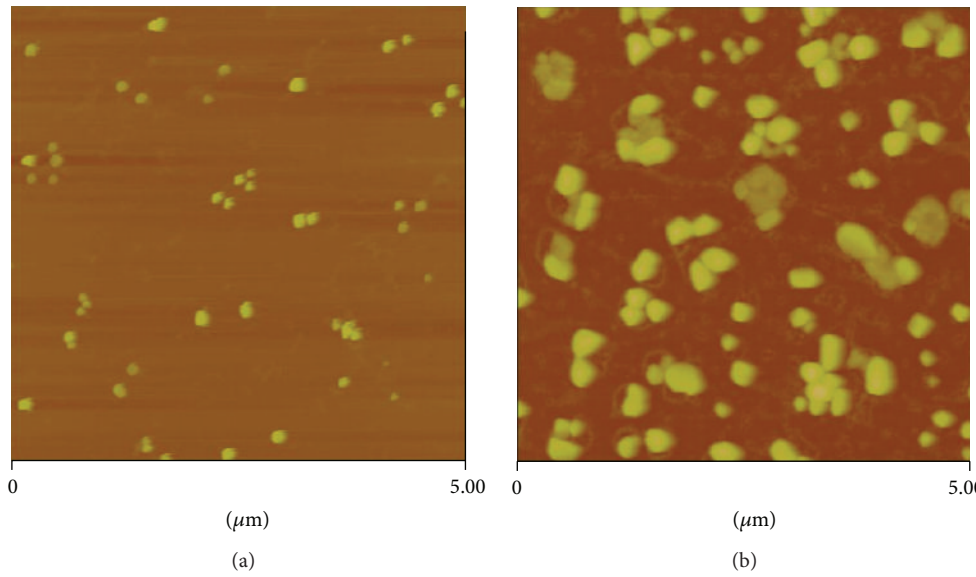

Figure 5: AFM images of DPG at different shearing rates. (The scanned area in Figure 6 is $5 \times 5\ \mu$m.).

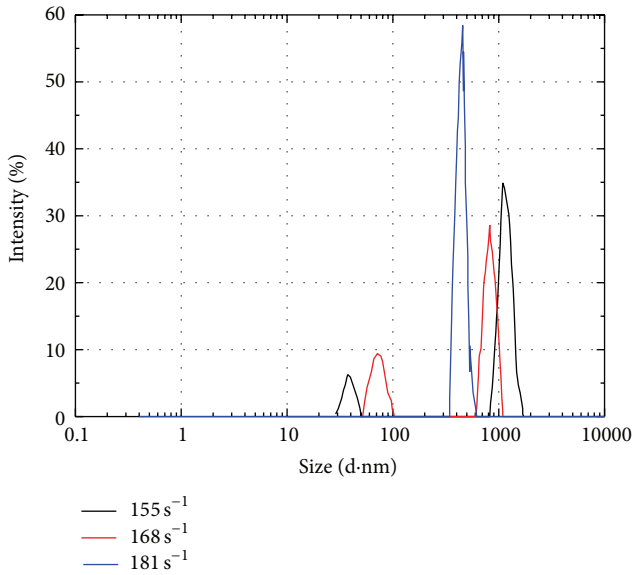

Figure 6: Particle size distribution curve of DPG at different shearing rates.

temperature, and γ_0 is a complicated function of surface potential given by

$$\gamma_0 = \frac{\exp\left(Ze\psi_0/2kT\right) - 1}{\exp\left(Ze\psi_0/2kT\right) + 1}, \quad (6)$$

where Z is the valence number of the particles in the diffuse layers, e is the charge number of the particles in the diffuse layers, and ψ_0 is the surface potential of the particles.

Formula (5) shows that the repulsion has a positive correlation with the particle size, the thickness of the diffuse electric double layers, and the surface potential. As the shearing rate decreases, the particle size of DPG increases. Cross-linking density is defined as the ratio of the number of cross-linked construction units to all of the construction units. If the particle size of DPG increases and the cross-linking density stays constant, then the repulsive and gravitational potential energies increase simultaneously, and the surface potential of the particles also increases. Formula (6) shows that the complicated function γ^0 of the surface potential changes within a small range; thus, the increase in the rate of the repulsive potential is smaller than that of the gravitational potential, which results in an enhanced attraction between the particles in the DPG system. As the shearing rate decreases, the gelation system is rarely influenced by the shearing action; thus, cross-linking opportunities and the cross-linking density increase; both the charge density of the DPG particles (the system has a negative charge) and surface potential decrease. All of the above factors lead to the decrease in the repulsive potential and the increase in attraction among the particles [15]. Thus, there is a trend toward aggregation among the DPG particles.

The particle size distribution curve of the DPG samples prepared at different shearing rates was obtained using DLS and is shown in Figure 6. The relationship between the hydrodynamic diameter of each DPG sample and its shearing rate is shown in Table 2. The average particle size of DPG decreases with an increase in shearing rate. At a greater shearing rate, the gelation system suffers more axial shearing stress, making the gelation system more easily broken, which leads to the decrease in the particle size of DPG.

The relationship between the hydrodynamic diameter of each DPG sample and its initial shearing rate is shown in Table 2.

3.1.3. The Effect of Salinity on the Morphology of DPG. The morphology of DPG was studied at various NaCl and $CaCl_2$ concentrations in the same gelation system (3000 mg·L^{-1} polymer and 500 mg·L^{-1} $Cr(Ac)_3$) at 30°C

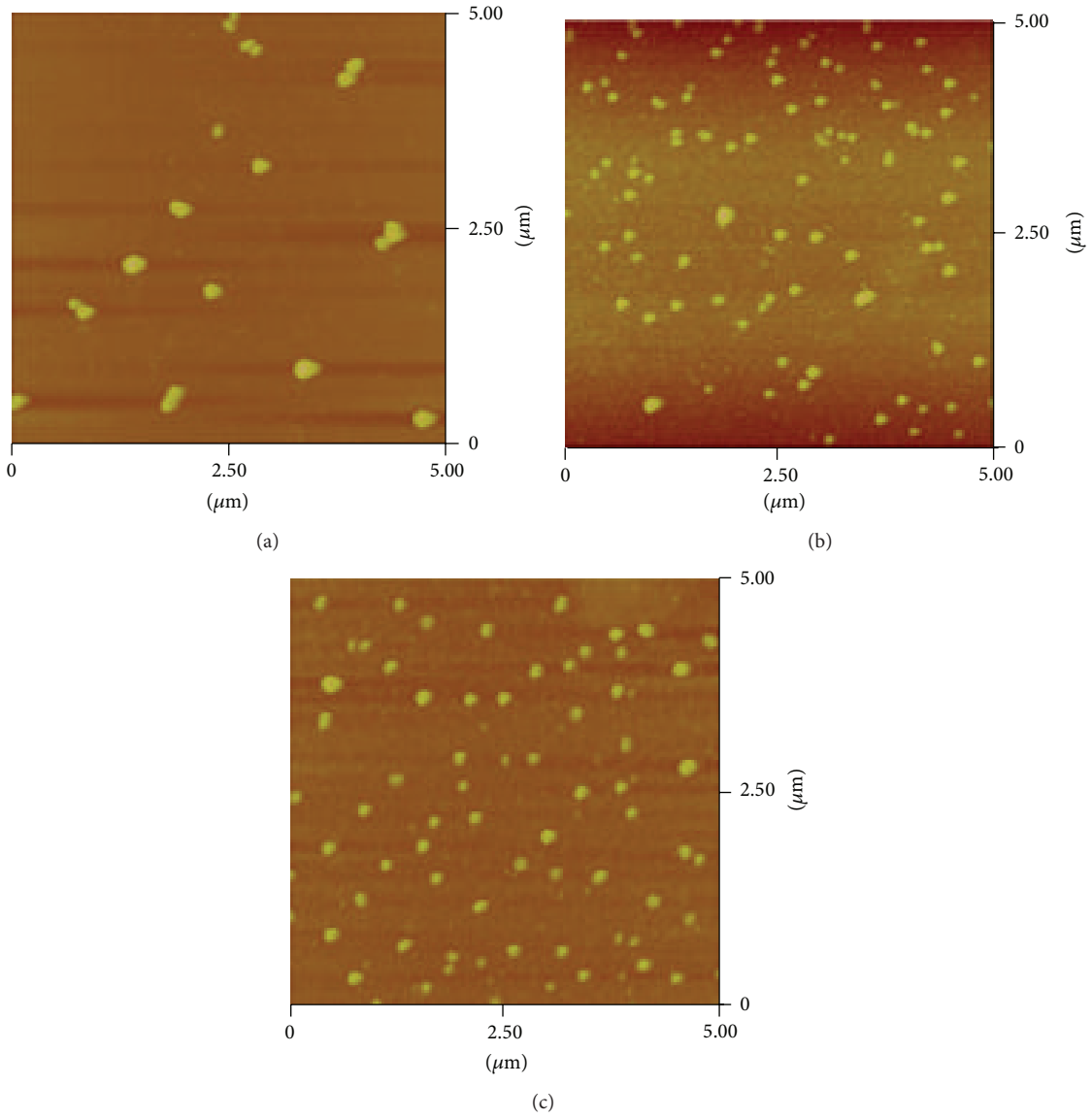

Figure 7: AFM images of DPG at various salinities.

Table 2: Relationship between the particle size of the gel dispersion and the average shear rate.

Items	Sample		
	1	2	3
Average shearing rate/s^{-1}	155	168	181
Particle size of DPG/nm	1100	750	410

and with a shearing rate of 181 s^{-1}. The DPG system was aged for 10 days before the variations in the morphology were studied. The results are shown in Figure 7.

As shown in Figure 7, the different concentrations and ion types have little influence on the morphology of DPG, which indicates that the system has an excellent resistance to salinity.

The DPG system generally has negative charges due to the adsorption by the polymer molecules at its surface. The ions and counter ions are both solvated; thus, there is a hydration film on the surface of DPG. The water molecules in the hydration film usually have an exact arrangement. When the gel particles approach each other, the hydration film is squeezed and deformed. The gravitational force that causes the exact arrangement tries to recover the original arrangement of the water molecules, which results in elasticity in the system [16]. Simultaneously, the viscosity of the water in the hydration film is larger than the viscosity of the free water in the system, which hinders the aggregation of DPG and stabilizes the system. When an electrolyte is added to the DPG system, it can cause coagulation of DPG. If the amount of the electrolyte is limited, it only compresses the diffuse electric double layer. Due to the existence of the hydration film, which acts as a buffer, the electrolyte only compresses the hydration film to a small extent without influencing the morphology of DPG.

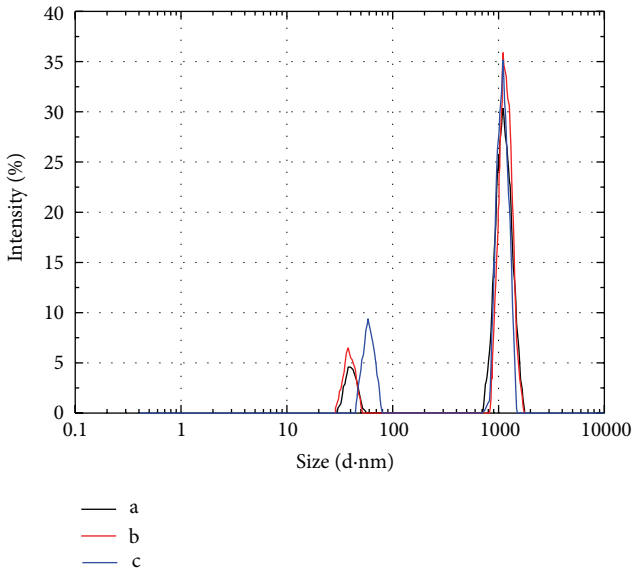

Figure 8: The effect of the salinity on the particle size of DPG. (a) In distilled water, (b) with 10,000 mg/L NaCl added, and (c) with 10,000 mg/L NaCl and 2000 mg/L $CaCl_2$ added.

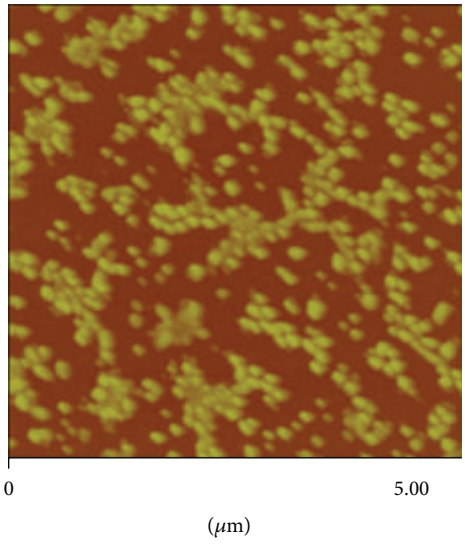

Figure 9: AFM photo of DPG after high-temperature aging. The scanned area is $5 \times 5\,\mu$m.

The particle size distribution curves of the DPG samples that were prepared at the different salinities at 30°C and aged for ten days (shown in Figure 7) were measured using DLS and are shown in Figure 8.

In Figure 8, there are two peaks in each of the particle size distribution curves of the three DPG samples. There is little variation among the second peaks, which are located at 1166 nm, 1132 nm, and 1100 nm. This suggests that an appropriate salinity has no effect on the particle size of DPG, which shows that DPG has a good tolerance to salinity. The DLS results are consistent with the AFM images of DPG.

3.1.4. The Effect of High Temperature on the Morphology of DPG. To study the influence of temperature, the DPG sample that was formed from 3000 $mg{\cdot}L^{-1}$ polymer and the 500 $mg{\cdot}L^{-1}$ $Cr(Ac)_3$ at 30°C and with a shearing rate of 181 s^{-1} was placed in an incubation chamber at 90°C for 15 days. The variations in this DPG system were studied, and the AFM images are shown in Figures 9 and 10 [13].

Figures 9 and 10 show that the DPG particles aggregate in large numbers at high temperatures. The particle size of DPG is small and the surface energy is high; thus, the DPG system tends to aggregate. Smaller particle sizes produce a greater effect. In a macroscopic view, the aggregation leads to some white insoluble floccus in the system.

According to the space stability theory, DPG can be regarded as gel particles that adsorb some polymer molecules on their surfaces; thus, there is a space repulsion potential energy in addition to the repulsive and gravitational potential energies between the particles. When DPG undergoes high-temperature aging, the Brownian movement of the particles increases and the chances of contact also increase such that the two cases shown in Figure 11 may occur.

When the DPG particles with adsorbed polymer layers touch each other, the high temperature leads to an increase in the thermal motion of the polymer molecules in the adsorbed layer, and the contact rate of polymer molecule chains increases, both of which lead to twining between the molecule chains and associations between the hydrophobic groups. Thus, overlap and penetration occur between the adsorbed layers. Moreover, as the particles become larger, their attraction to other particles increases, which accelerates the aggregation of DPG.

Figure 9 shows that DPG has a good temperature resistance and does not degrade or dehydrate during a high-temperature aging process at 90°C. Thus, we can take advantage of the adhesion and aggregation properties of DPG at high temperatures and use it to plug deep reservoirs in practical applications.

The particle size distribution curves were measured using DLS before and after aging at 90°C for 15 days and are shown in Figures 12 and 13. After aging at high temperatures, the value of the characteristic peak changes from 400 nm to three different characteristic peaks at 186.6, 796.2, and 4450 nm. DPG tends to aggregate at high temperatures, which makes the particle size larger and is consistent with previous results on the morphology of DPG. The flocculation is the DPG aggregates of largest particle sizes (over 5 μm).

4. Conclusions

(1) AFM studies show that DPG is made of small pseudospherical particles and that the particle size can be controlled by adjusting the shearing rate. The particles of DPG have a ratio between their major and minor axis lengths close to 1. As the shearing rate increases, the ratio approaches 1. Higher initial polymer mass concentrations result in larger DPG particle sizes. Salinity has a minor effect on the micromorphology, and an aggregation phenomenon occurs with aging.

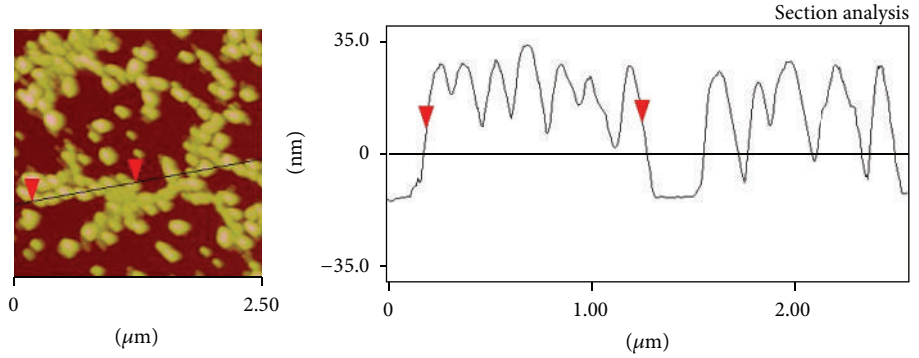

Figure 10: Section analysis of DPG after high-temperature aging.

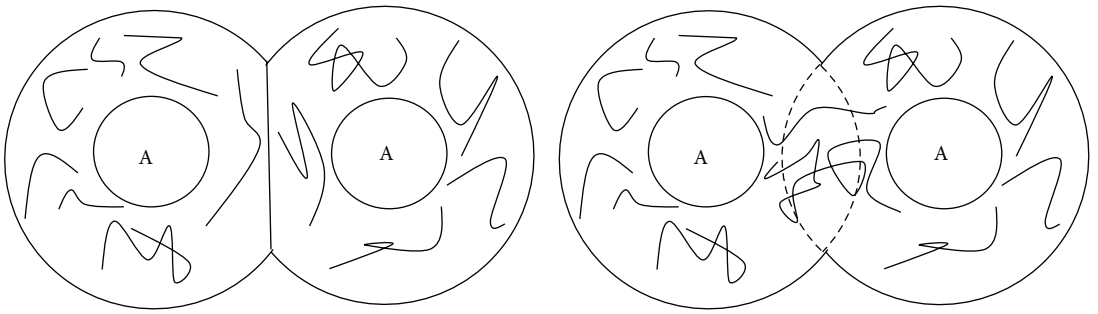

(a) The adsorbed layer is compressed (b) The adsorbed layer is interpenetrative

Figure 11: The interaction between two DPG particles with adsorbed polymer layers.

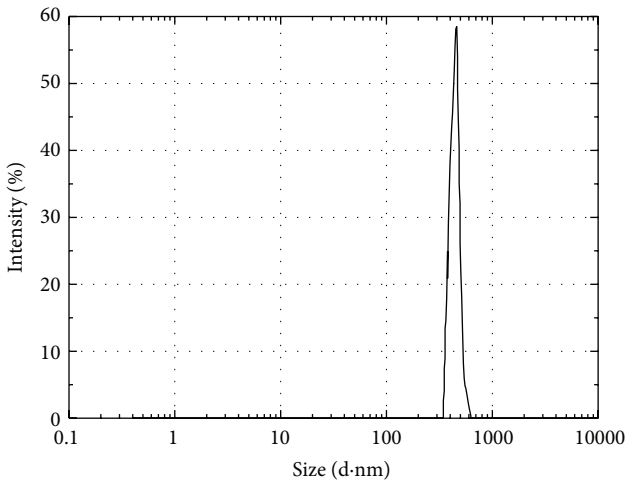

Figure 12: The particle size distribution curve of DPG before high-temperature aging.

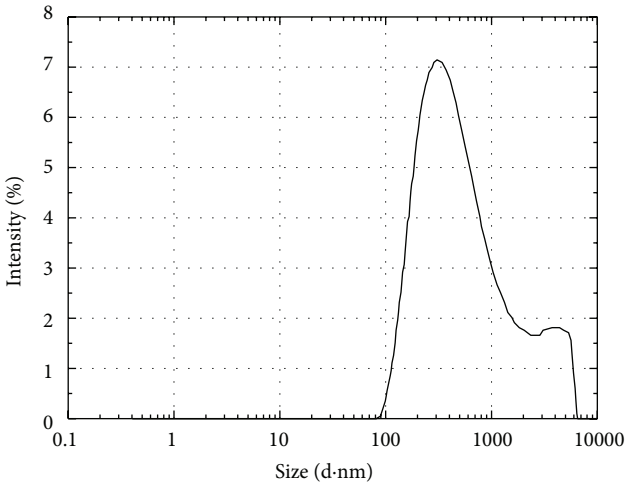

Figure 13: The particle size distribution curve of DPG after high-temperature aging.

(2) DLS studies of the effects of the initial polymer mass concentration, the shearing rate, the salinity, and the high-temperature aging on the particle size of DPG are consistent with the AFM results.

(3) Using the DLVO theory and the space stability theory, this paper clarifies the factors that make DPG aggregate easily. The easy aggregation is the result of a synergistic effect that includes the gravitational potential energy E_A, the repulsive potential energy E_R, and the space repulsive potential E_R^s.

(4) The morphology of DPG and the factors that influence the morphology are studied in this paper to provide a scientific basis and technical support for the IOR mechanism of DPG and its application in the field.

Conflict of Interests

The authors declare that they have no conflict of interests regarding the publication of this paper.

Acknowledgments

This paper was supported by the Fundamental Research Funds for the Central Universities (no. 2-9-2014-007), the National Natural Science Foundation of China (no. 51174221), and the Program for New Century Excellent Talents in University (no. 20110226).

References

[1] X. F. Tang, Q. Wu, G. H. Liu, S. R. Gu, and H. Y. Li, "Field test on integral modifying and flooding project in regional reservoir with weak gel," *Acta Petrolei Sinica*, vol. 24, no. 4, pp. 58–61, 2003.

[2] J. H. Liu and T. X. Ye, "Study on the valuation of low concentration HPAM/AlCit system and its gelation influencing factors," *Chemical Engineering of Oil and Gas*, vol. 3, pp. 375–378, 2003.

[3] H. Frampton, J. C. Morgan, S. K. Cheung, L. Munson, and K. T. Chang, "Development of a novel waterflood conformance control system," in *Proceedings of the SPE/DOE 14th Symposium on Improved Oil Recovery (IOR '04)*, Tulsa, Ok, USA, 2004.

[4] J. Pritchett, H. Frampton, J. Brinkman et al., "Field application of a new in-depth waterflood conformance improvement tool," in *Proceedings of the SPE International Improved Oil Recovery Conference in Asia Pacific (IIORC '03)*, pp. 365–372, Kuala Lumpur, Malaysia, October 2003, SPE 84897.

[5] A. Omari, G. Chauveteau, and J. Rose, "New size-controlled microgels for oil production," in *Proceedings of the SPE International Symposium on Oilfield Chemistry*, pp. 1–8, Houston, Tex, USA, February 2001.

[6] D. Rousseau, G. Chauveteau, M. Renard et al., "Rheology and transport in porous media of new water shutoff/conformance control microgels," in *Proceeding of the SPE International Symposium on oilfield Chemistry*, The Woodlands, Tex, USA, February 2005.

[7] A. Zaitoun, R. Tabary, D. Rousseau et al., "Using microgels to shut off water in a gas storage well," in *Proceedings of the SPE International Symposium on Oilfield Chemistry*, vol. 106042, pp. 221–228, Houston, Tex, USA, March 2007.

[8] J. P. Coste, "In-depth fluid diversion by pre-gelled particles," in *Proceedings of the SPE/DOE Improved Oil Recovery Symposium*, SPE 59362, Laboratory Study and Pilot Testing, Tulsa, Okla, USA, April 2000.

[9] B. J. Bai, "Case study on prefromed particle gel for in-depth fluid diversion," in *Proceedings of the SPE Symposium on Improved Oil Recovery*, SPE-113997-MS, Tulsa, Okla, USA, April 2008.

[10] H. W. Ma, Y. Z. Liu, and Y. K. Li, "Research on flexible particle migration in porous media," *Oil Drilling & Production Technology*, vol. 4, pp. 80–82, 2007.

[11] Q. You, Y. C. Tang, and C. L. Dai, "Research on a new profile control agent: dispersed particle gel," in *Proceedings of the SPE Enhanced Oil Recovery Conference*, SPE 143514, Kuala Lumpur, Malaysia, July 2011.

[12] F. L. Zhao, *Principle of Enhanced Oil Recovery*, China University of Petroleum Press, Dongying, China, 2006.

[13] Q. You, C. L. Dai, and Y. C. Tang, "Study on performance evaluation of dispersed particle gel for improved oil recovery," *Journal of Energy Resources Technology*, vol. 135, no. 4, Article ID 042903, 7 pages, 2013.

[14] J. S. Qin and A. F. Li, *Reservoir Physics*, China University of Petroleum Press, Dongying, China, 2nd edition, 2006.

[15] K. Chen, *Study on Preparation, Performance Evaluation and Application of Microgel*, China University of Petroleum Press, Dongying, China, 2007.

[16] Z. Sheng, Z. G. Zhao, and G. T. Wang, *Colloid and Surface Chemistry*, Chemical Industry Press, Beijing, China, 2012.